Materials Chemistry

PAPER

Alloying to increase the band gap for improving thermoelectric properties of Ag$_2$Te

Yanzhong Pei, Nicholas A. Heinz and G. Jeffrey Snyder*

Ag$_2$Te simultaneously shows high mobility and low thermal conductivity, however the relatively low band gap of ~0.2 eV prevents it from achieving high thermoelectric figure of merit, zT, in the high temperature phase. In this study, the band gap of Ag$_2$Te has been increased enabling a zT of unity by forming alloys and composites with PbTe, thereby demonstrating the importance of exploiting potentially good thermoelectrics among these small band gap semiconductors and similar materials.

Introduction

To make highly efficient thermoelectric devices for power generation or refrigeration, the most challenging aspect is to increase the thermoelectric figure of merit (zT) of a thermoelectric material. The transport properties including resistivity (ρ), Seebeck coefficient (S), electronic (κ_E) and lattice (κ_L) components of thermal conductivity ($\kappa = \kappa_E + \kappa_L$) determine the figure of merit, $zT = S^2T/\rho\kappa$, where T is absolute temperature.

Virtually none of these properties can be independently tuned as an effective approach for high zT because they are strongly coupled to each other.[1,2] However, the thermoelectric power factor, which characterizes the electrical properties, is known to be a function of effective mass (m^*) and mobility (μ)[1,3–5] *via* the weighted mobility[3,4,6,7] ($S^2/r \propto m^{*1.5}\mu$). A further consideration of multi-valley band systems and carrier scattering by acoustic vibrations,[8–10] as found in most efficient thermoelectrics at temperatures where zT peaks, reveals that large number of valleys (N_v)[3,4,11,12] and low conduction mass (m_c^*) are beneficial for thermoelectric performance ($S^2/\rho \propto N_v/m_c^*$).[3,4,13–15]

In spite of the low degeneracy, it has long been known that narrow band gap Γ-semiconductors ($N_v = 1$) such as InSb and InAs contain a power factor as high or even higher[16,17] than those of known high degeneracy n-type thermoelectrics[18] ($N_v \geq 4$), because of the extremely low effective masses ($\leq 0.05 m_e$, where m_e is the free electron mass).[19] However, very few studies have shown $zT > 0.5$ in these materials, because of the strong detrimental effects of minority carriers due to the small gap and/or the high thermal conductivity[16,20] (~20 W m^{-1} K^{-1} at 300 K).

Being similar to the above mentioned compounds, another known Γ-semiconductor,[21,22] Ag$_2$Te, also shows very low effective mass[23] leading to high mobility. In addition, the intrinsic low thermal conductivity[24] has inspired research interest in this system as a thermoelectric material,[25–27] and a maximum zT of

~0.6 was achieved.[26] Due to the small band gap (≤ 0.2 eV, depending on the phase modification) of this material,[23,28] the observed nearly intrinsic conduction (decreasing or flattening S with increasing T)[23,26,29] behavior strongly suggests that the potential of this material as a thermoelectric is not fully realized.

One approach to reduce the negative effects from the minority carriers is to increase the band gap,[1,3,5] especially at high temperatures. In the present study, formation of an alloy between Ag$_2$Te and PbTe is utilized to achieve a band gap wide enough to fully realize the potential of this material as an efficient thermoelectric. This is motivated not only by the high solubility at high temperatures (needed to increase the band gap), but also by its strong temperature dependence, enabling fine precipitates to be formed during the low temperature synthesis.[30,31] This may additionally scatter phonons, targeting a further reduction of the thermal conductivity.[30–32] Using this route we show significantly higher zT near unity which emphasizes the importance of increasing the band gap of these narrow-gap semiconductors as thermoelectrics.

Experimental methods

According to the Ag$_2$Te-PbTe pseudo-binary phase diagram,[33–35] as shown in Fig. 1, compositions of (PbTe)$_x$(Ag$_2$Te)$_{1-x}$ with $x = 0$, 0.05, 0.10 and 0.15 were synthesized by melting (1273 K for 6 h), quenching (in cold water), and annealing (at 700 K for 3 days) methods in vacuum sealed quartz ampoules. Hot pressed (700 K for 1 h) pellets with a theoretical density $\geq 98\%$ were used for thermoelectric transport property measurements. In attempt to tune the carrier concentration, another $x = 0.10$ sample ($x = 0.10$-Ag) was also synthesized using 0.02% at. deficiency of Ag: (PbTe)$_x$(Ag$_{1.9996}$Te)$_{1-x}$. The resistivity and Hall coefficient (R_H) were simultaneously measured using the Van der Pauw technique under a reversible magnetic field of 2T. The Seebeck coefficient was obtained from the slope of the thermopower *vs.* temperature gradient using Chromel-Nb thermocouples.[36] Thermal diffusivity (D) was measured by the laser flash method (Netzsch LFA

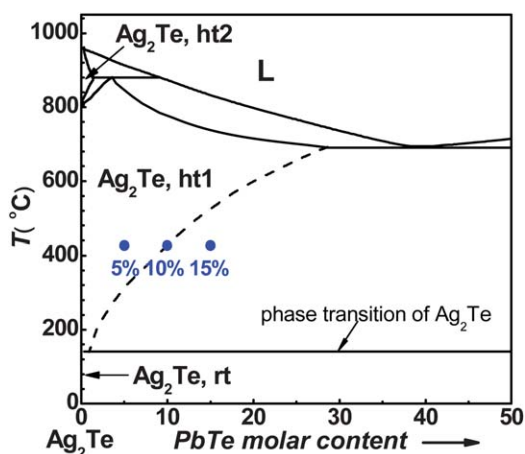*Materials Science, California Institute of Technology, Pasadena, CA, 91125, USA. E-mail: jsnyder@caltech.edu*

18256 | *J. Mater. Chem.*, 2011, **21**, 18256–18260

This journal is © The Royal Society of Chemistry 2011

Fig. 1 The $(PbTe)_x(Ag_2Te)_{1-x}$ pseudo-binary phase diagram.[37] A high solubility of PbTe in Ag_2Te enables a band gap wide enough for utilization at high temperatures for thermoelectric applications. The strong temperature dependent solubility supports precipitate growth below the eutectic temperature.[33–35] The points shown are the compositions and final annealing temperatures used in this study, which are quenched from the melt at 1273 K.

457). A Dulong-Petit value ($3k_B$ per atom) of heat capacity (C_p) is used to determine the thermal conductivity *via* $k = dC_pD$, where d is the density measured using the mass and geometric volume of the pellet. The combined uncertainty for the determination of zT is ~20%. X-ray diffraction and scanning electron microscopy (SEM) were use to characterize the phase composition (EDS) and microstructure.

Results and discussion

The result of microstructure analysis on the as quenched ingots having $x = 0.05$ and 0.10 are shown in Fig. 2 a and b. As can be

seen, the ~1 μm sized PbTe precipitates (white) are homogenously dispersed into the Ag_2Te matrix. This indicates the formation of PbTe precipitates upon cooling. Composition determination shows ~48% at. Pb and ~3% at. Ag in the PbTe inclusions, and ~66.7% at. Ag and <~1% Pb in the matrix Ag_2Te phase. Precipitate aggregation can be also found at the grain boundaries. Typically the volume fraction of precipitates can be well controlled by tuning the initial composition.[31]

Precipitate coarsening can be found by comparing the structures obtained by quenching and annealing for 3 days at 700 K (Fig. 2 c and d). The PbTe precipitates grow to several microns in size, presumably due to the fast diffusion of Pb in vacancy structured Ag_2Te (cubic phase at high temperatures).[34] All these features suggest the alloy is formed rapidly as the temperature is raised and the solid solution quickly precipitates with decreasing temperature. This results in complex composition and temperature dependent thermoelectric transport properties.

The measured transport properties such as resistivity, Seebeck coefficient, Hall carrier concentration ($n_H = 1/eR_H$, e is the electron charge) and Hall mobility ($\mu_H = R_H/\rho$) are shown in Fig. 3 a, b, c and d. Abnormalities in the data can be seen at ~400 K in all the electrical transport properties and thermal conductivity as well (Fig. 4). This is due to the low temperature monoclinic to high temperature cubic phase transition of Ag_2Te. The influence of such a phase transition on the transport properties has been well studied.[38–40]

With the addition of PbTe, the slight increase in resistivity can be ascribed to the slight decrease in Hall mobility, resulting from the PbTe precipitates, as the Hall carrier concentration for majority of the samples remains unchanged.

It should be noted that the Hall carrier concentration is calculated form the measured Hall coefficient *via* $n_H = 1/eR_H$. The actual extrinsic carrier concentration is determined by the defect or doping concentration, and usually is independent of temperature[30,41] as long as such impurities are fully ionized,
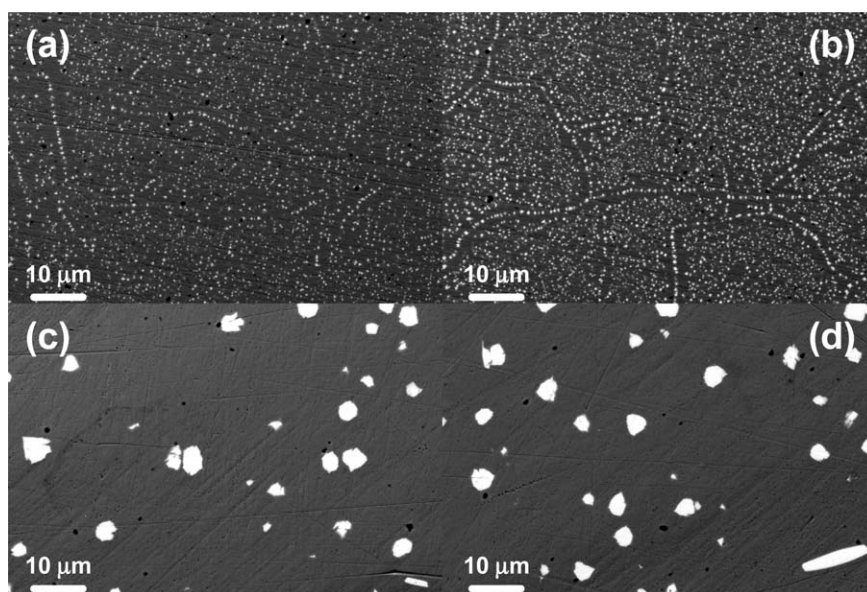

Fig. 2 The microstructure for as-quenched (a and b) and annealed (c and d) samples having $x = 0.05$ (a and c) and $x = 0.10$ (b and d), taken under backscattering mode. Precipitates are coarsened from ~1 μm to several μm by post-annealing at 700 K for 3 days.
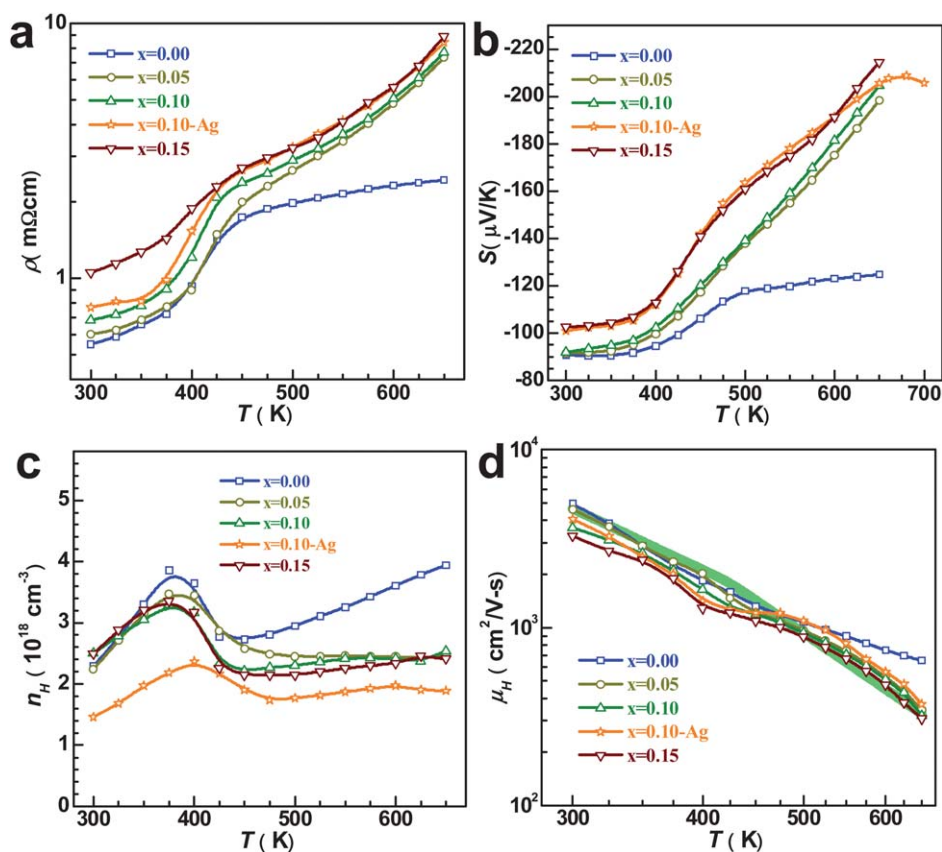
Fig. 3 Temperature dependent electrical transport properties including resistivity (a), Seebeck coefficient (b), Hall carrier concentration (c) and Hall mobility (d). The observed abnormalities at ~400 K for each property are due to the monoclinic (low temperature) → cubic (high temperature) phase transition of Ag_2Te. The temperature dependent mobility shows good consistency with the predicted (solid line, d) trend for an acoustic scattering mechanism taking temperature dependent effective mass into account.

meaning, an approximately constant R_H with increasing temperature. However, due to the thermally excited electron-hole pairs, especially in narrow band gap semiconductors and at high temperatures, minority carriers contribute to the transport and lead to a compensation (decreasing) Hall coefficient, ultimately leading to an increase of n_H.[42]

This does not necessarily mean the extrinsic doping is increased in the current study. With a very small band gap of ~0.05 eV for the low temperature phase[23,28] (only 2 k_BT at 300 K, k_B being the Boltzmann constant), there should be a large quantity of minority holes since the full width half maximum (FWHM) of the Fermi distribution is ~4 k_BT. For this reason, the increase of n_H, or more precisely, the decrease of R_H, at $T < 400$ K, is due to the compensation by minority carriers. Similar to the n_H increasing at $T < 400$ K, the continuous increase of n_H found in the high temperature phase for the sample with $x = 0$ (Fig. 3c), is also due to the minority carriers even though the band gap increases from ~0.05 eV for the low temperature phase to ~0.2 eV for the high temperature cubic phase.[21,43] The activation of minority carriers also explains the observed flattening of the Seebeck coefficient versus temperature for the $x = 0$ sample (Fig. 3b), and the slower increase in resistivity for $x = 0$ in the high temperature phase (Fig. 3a).

The addition of PbTe changes the temperature dependences of all the electrical transport properties at $T > 400$ K. The nearly constant Hall carrier concentration, and the approximately

linearly increasing Seebeck coefficient with increasing temperature, suggests this material behaves similarly to traditional good thermoelectric materials showing degenerate semiconductor behavior. With a PbTe solubility of about 8–12% mol.[33–35] in Ag_2Te at ~700 K, the high temperature transport properties can be explained base on an alloy phase in this study.

The reason for the Ag_2Te-PbTe alloys having different electrical properties can be attributed to an increase in the band gap, which reduces the influence of minority carriers. Utilizing the Goldsmid method,[44] the Seebeck coefficient measurement for a simple band structure system such as Ag_2Te[21,22] enables a determination of the effective band gap via $E_g = 2eS_{max}T_{max}$, where S_{max} and T_{max} are the maximum Seebeck coefficient and the temperature at which S_{max} occurs. This yields a band gap of 0.28 eV for the sample with $x = 0.10$ at ~650 K. Literature data showing maximum Seebeck coefficients of Ag_2Te enables an estimation of $E_g = 0.04$eV for the low temperature phase[28] and $E_g = 0.2$eV for the high temperature phase.[29] The values for E_g obtained by this method for both high and low temperature phases are excellently consistent with those determined by other methods.[21,23,28,43] Therefore, the resulting band gap of 0.28 eV (greater than 5 k_BT in this study) enables the degenerate semiconducting behavior by preventing the activation of minority carriers.

It was known that carrier scattering in Ag_2Te was dominated by acoustic phonons in both low temperature and high

18258 | J. Mater. Chem., 2011, **21**, 18256–18260

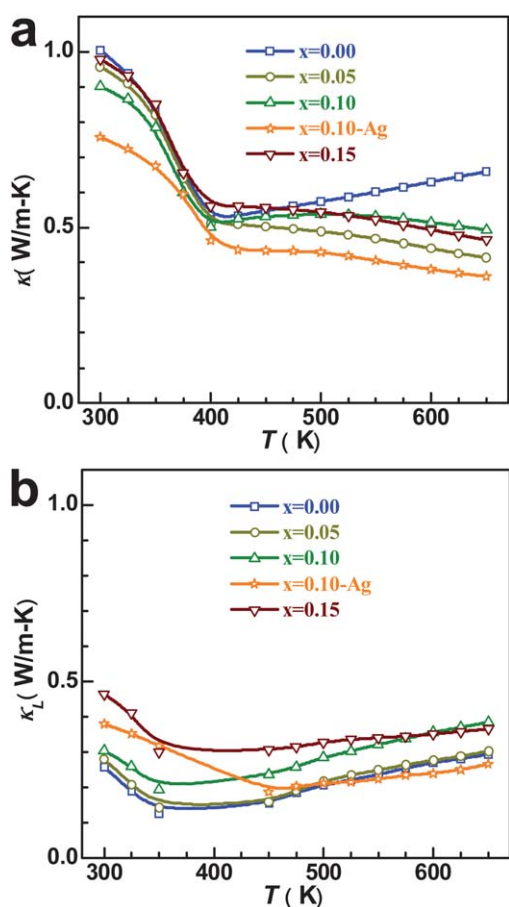This journal is © The Royal Society of Chemistry 2011

Fig. 4 Total thermal conductivity (a) and the lattice component (b) as a function of temperature. The lattice thermal conductivity shows glassy behavior and is close to the amorphous limit value of ~0.3 W m⁻¹ K⁻¹ in the entire temperature investigated.

temperature phases.[38,45,46] The existence of acoustic scattering can be seen from the rapidly decreasing Hall mobility with increasing temperature (Fig. 3d). Furthermore, the bands for narrow gap Ag_2Te were also found to be nonparabolic and could be described by a Kane band model.[38,45–47] Nonparabolic Kane band theory[14,48] and acoustic scattering theory[8,9] enables a detailed single Kane band model (SKB)[14,48,49] to predict the electrical transport properties of a thermoelectric semiconductor. Using the above mentioned E_g and the measured electrical transport shown in Fig. 3, the SKB model yields small effective mass (<0.1 m_e) for these materials, which increases with increasing temperature via $d\ln m^*/d\ln T = 0.5$ and $d\ln m^*/d\ln T = 1$ for the low and high temperature phases. Such an increase in effective mass is very similar to PbTe[14,30,50] having nonparabolic bands. Knowing the temperature dependent effective mass, the theoretical temperature dependent mobility can be predicted as seen by the solid line in Fig. 3d for acoustic scattering. The excellent consistency between the measured and predicted temperature dependence of mobility further confirms the idea that carrier scattering is dominated by acoustic phonons in these materials. The obtained deformation potential coefficient, which defines the strength of carrier scattering by acoustic phonons, is found to be about 21 eV and 32 eV for low and high temperature phases assuming an isotropic conduction band.

The total thermal conductivity (κ) and its lattice component (κ_L) are shown in Fig. 4 a and b, respectively. κ for Ag_2Te in this study shows good consistency with the literature data[26] where the resistivity was similar to that of this work. It should be noted that the lattice thermal conductivity is obtained by subtracting the electronic contribution (κ_E) from the total thermal conductivity, where κ_E is determined by LT/ρ with the Lorenz number (L) calculated from the above SKB model.[14,48,49]

With the addition of PbTe into Ag_2Te, the fine microstructure obtained (Fig. 2) is generally of interest for thermoelectrics because of expected phonon scattering at the interfaces.[30,31] However, this effect is not very significant in this study, due to the intrinsically low κ_L of ~0.3 W m⁻¹ K⁻¹ (Fig. 4b) in the Ag_2Te matrix material.

Ag_2Te intrinsically has low thermal conductivity due to the highly disorder structure of the Ag atoms.[51,52] The Ag atoms in the high temperature phase are highly mobile with liquid-like diffusion coefficient.[53,54] This mechanism is effective in producing low thermal conductivity materials for thermoelectrics such as Cu_2Se,[55] Zn_4Sb_3[56] and AgCrSe.[57] With the measured longitudinal and transverse sound velocities of 3900 and 1200 m s⁻¹, the κ_L for all the materials obtained in this study are comparable to the amorphous limit of ~0.3 W m⁻¹ K⁻¹ in the entire temperature range, according to the Debye and Cahill model.[58] The intrinsically low κ_L can be partially explained by the very low mean sound velocity of 1360m s⁻¹ (meaning a Debye temperature of 143 K), and is possibly due to the highly anharmonic vibrations in these ionically conducting and disordered materials. The high mobility of the Ag may lead to difficulties operating thermoelectric generators due to electromigration as was the case for Cu_2Se thermoelectric material. However, formation of $Ag_{2-x}K_xTe$ or $Ag_{2-x}Na_xTe$ alloys may reduce the conduction of Ag^+ because K_2Te and Na_2Te have at least twice higher activation energies for ionic conduction among all (Li, Na, K, Cu, $Ag)_2Te$ compounds.[21]

The temperature dependent zT is shown in Fig. 5. An effective increase in the band gap, with a combination of intrinsic low lattice thermal conductivity, actually leads to a $zT \sim 0.9$ in the $x = 0.05$ sample and with better carrier concentration tuning,
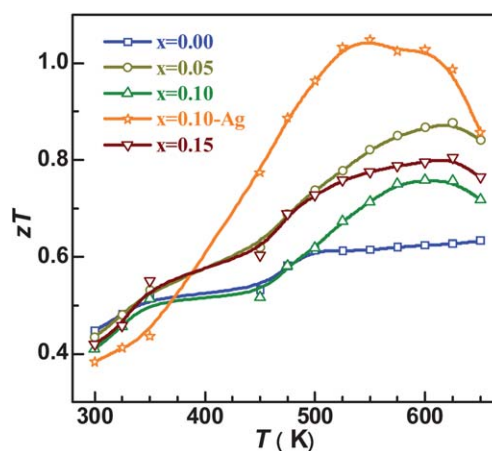

Fig. 5 The thermoelectric figure of merit (zT) as a function of temperature, showing a maximum zT of approximately unity in the range of 500–600 K.

$zT \sim 1$ in the $x = 0.10$-Ag sample (Fig. 3c). It should also be noted that the zT curve is less temperature dependent than conventional thermoelectric materials, which enables high average zT for large device efficiency.

Summary

In summary, the narrow band gap semiconductor Ag_2Te is improved to make a competitive thermoelectric material by increasing the band gap through alloying and composite formation with PbTe. A further combination of intrinsically low lattice thermal conductivity enables a zT of unity, emphasizing the necessary exploitation of this and other similar materials for potential thermoelectric applications.

Acknowledgements

References

1 A. F. Ioffe, *Semiconductor thermoelements, and Thermoelectric cooling*, Infosearch, London, 1957.
2 G. J. Snyder and E. S. Toberer, *Nat. Mater.*, 2008, **7**, 105–114.
3 H. J. Goldsmid, *Thermoelectric refrigeration*, Plenum Press, New York, 1964.
4 R. P. Chasmar and R. Stratton, *J. Electronics Control*, 1959, **7**, 52–72.
5 H. J. Goldsmid, *Applications of thermoelectricity*, Methuen, New York, 1960.
6 G. A. Slack, in *CRC handbook of thermoelectrics*, ed. D. M. Rowe, CRC Press, Boca Raton, Fla., 1995, pp. 406–440.
7 G. D. Mahan, in *Solid State Physics*, ed. H. Ehrenreich and F. Spaepen, Academic Press Inc, San Diego, 1998, pp. 81–157.
8 J. Bardeen and W. Shockley, *Phys. Rev.*, 1950, **80**, 72–80.
9 C. Herring and E. Vogt, *Phys. Rev.*, 1956, **101**, 944–961.
10 J. M. Ziman, *Electrons and Phonons: The Theory of Transport Phenomena in Solids*, Oxford, Clarendon, 1960.
11 Y. Pei, X. Shi, A. LaLonde, H. Wang, L. Chen and G. J. Snyder, *Nature*, 2011, **473**, 66–69.
12 C. M. Bhandari and D. M. Rowe, in *CRC handbook of thermoelectrics*, ed. D. M. Rowe, CRC Press, Boca Raton, Fla., 1995, pp. 43–53.
13 H. J. Goldsmid, *Introduction to Thermoelectricity*, Springer, Heidelberg, 2009.
14 Y. I. Ravich, B. A. Efimova and I. A. Smirnov, *Semiconducting Lead Chalcogenides*, Plenum Press, New York, 1970.
15 R. W. Ure and R. R. Heikes, in *Thermoelectricity: science and engineering*, ed. R. R. Heikes and R. W. Ure, Interscience Publishers, New York, 1961, pp. 339–338.
16 F. D. Rosi, E. F. Hockings and N. E. Lindenblad, *Rca Rev.*, 1961, **22**, 82–121.
17 S. Yamaguchi, T. Matsumoto, J. Yamazaki, N. Kaiwa and A. Yamamoto, *Appl. Phys. Lett.*, 2005, **87**, 201902.
18 D. M. Rowe, *CRC handbook of thermoelectrics*, CRC Press, Boca Raton, Fl., 1995.
19 New Semiconductor Materials. Characteristics and Properties http://www.ioffe.ru/SVA/NSM/Semicond/index.html.
20 Y. Pei and D. Morelli, *Appl. Phys. Lett.*, 2009, **94**, 122112.
21 H. Kikuchi, H. Iyetomi and A. Hasegawa, *J. Phys.: Condens. Matter*, 1998, **10**, 11439–11448.
22 S. Kashida, N. Watanabe, T. Hasegawa, H. Iida and M. Mori, *Solid State Ionics*, 2002, **148**, 193–201.
23 C. Wood, W. Kane and V. Harrap, *Phys. Rev.*, 1961, **121**, 978.
24 P. Taylor and C. Wood, *J. Appl. Phys.*, 1961, **32**, 1.
25 M. Fujikane, K. Kurosaki, H. Muta and S. Yamanaka, *J. Alloys Compd.*, 2005, **393**, 299–301.
26 J. Capps, F. Drymiotis, S. Lindsey and T. M. Tritt, *Philos. Mag. Lett.*, 2010, **90**, 677–681.
27 J. Capps, B. Ma, T. Drye, C. Nucklos, S. Lindsey, D. Rhodes, Q. Zhang, K. Modic, S. Cawthorne and F. Drymiotis, *J. Alloys Compd.*, 2011, **509**, 1544–1549.
28 R. Dalven and R. Gill, *Phys. Rev.*, 1966, **143**, 666.
29 M. Fujikane, K. Kurosaki, H. Muta and S. Yamanaka, *J. Alloys Compd.*, 2005, **387**, 297–299.
30 Y. Pei, A. F. May and G. J. Snyder, *Adv. Energy Mater.*, 2011, **1**, 291–296.
31 Y. Pei, J. Lensch-Falk, E. S. Toberer, D. L. Medlin and G. J. Snyder, *Adv. Funct. Mater.*, 2011, **21**, 241–249.
32 M. G. Kanatzidis, *Chem. Mater.*, 2010, **22**, 648–659.
33 B. Grieb, E. Lugscheider and J. Wilden, *Ternary Alloys, VCH*, 1988, **2**, 465–476.
34 K. Bergum, T. Ikeda and G. Jeffrey Snyder, *J. Solid State Chem.*, 2011, **184**, 2543–2552.
35 R. Blachnik and B. Gather, *J. Less Common Met.*, 1978, **60**, 25–32.
36 S. Iwanaga, E. S. Toberer, A. D. LaLonde and J. G. Snyder, *Rev. Sci. Instrum.*, 2011, **82**, 063905.
37 F. Wald, *J. Less Common Met.*, 1967, **13**, 579–590.
38 S. Aliev and Z. Agaev, *Semiconductors*, 2007, **41**, 1027–1032.
39 S. Aliev, *Semiconductors*, 2004, **38**, 796–799.
40 F. Aliev, *Inorg. Mater.*, 2002, **38**, 995–997.
41 R. F. Pierret, *Advanced semiconductor fundamentals*, Pearson Education, Upper Saddle River, N.J., 2003.
42 E. H. Putley, *The Hall effect and related phenomena*, Butterworths, London, 1960.
43 V. D. Nguyen and N. Pham, *Phys. Status Solidi B*, 1968, **30**, 557–567.
44 H. Goldsmid and J. Sharp, *J. Electron. Mater.*, 1999, **28**, 869–872.
45 M. Jafarov, *Semiconductors*, 2010, **44**, 1280–1284.
46 F. Aliev, M. Jafarov, G. Askerova and E. Gojaev, *Semiconductors*, 2010, **44**, 1008–1011.
47 S. Aliev, U. Suyunov, D. Arasly and M. Aliev, *Soviet physics Semiconductors*, 1973, **7**, 737–740.
48 Y. I. Ravich, B. A. Efimova and V. I. Tamarche, *Phys. Status Solidi B*, 1971, **43**, 11–33.
49 C. M. Bhandari and D. M. Rowe, in *CRC handbook of thermoelectrics*, ed. D. M. Rowe, CRC Press, Boca Raton, Fla., 1995, pp. 27–42.
50 H. A. Lyden, *Phys. Rev.*, 1964, **135**, A514–A521.
51 T. Sakuma and S. Saitoh, *J. Phys. Soc. Jpn.*, 1985, **54**, 3647–3548.
52 J. Schneider and H. Schulz, *Z. Kristallogr.*, 1993, **203**, 1–15.
53 H. Okazaki, *J. Phys. Soc. Jpn.*, 1977, **43**, 213–221.
54 M. Kobayashi, K. Ishikawa, F. Tachibana and H. Okazaki, *Phys. Rev. B*, 1988, **38**, 3050–3055.
55 E. F. Hampl, Jr, United States Patent 3853632, 1974.
56 G. Snyder, M. Christensen, E. Nishibori, T. Caillat and B. Iversen, *Nat. Mater.*, 2004, **3**, 458–463.
57 F. Gascoin and A. Maignan, *Chem. Mater.*, 2011, **23**, 2510–2513.
58 D. G. Cahill and R. O. Pohl, *Annu. Rev. Phys. Chem.*, 1988, **39**, 93–121.